Dissolved molybdenum asymptotes in sulfidic waters
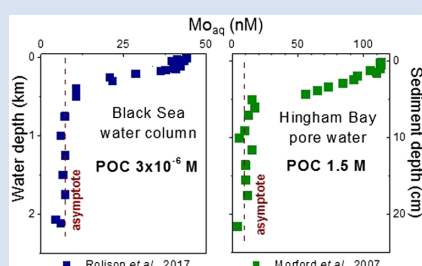
G.R. Helz[*]

OPEN ACCESS

Abstract

Molybdenum enrichment in organic-rich sediments is well known and is an accepted proxy for sulfidic conditions during sedimentation, but debate persists about how Mo enrichment arises. Organic scavenging and sulfide precipitation are the processes most often invoked. When dissolved Mo (Mo_{aq}) precipitates solely within sulfidic pore waters of sediments, contiguous particulate organic carbon concentrations (POC) are orders of magnitude higher than when it precipitates in euxinic water columns. Nevertheless, in both cases, Mo_{aq} concentrations decline until reaching quite similar asymptotes centred around 7.8 nM. That Mo_{aq} asymptotes are independent of organic carbon availability is inconsistent with organic scavenging as the dominant Mo fixing mechanism. In contrast, the $FeMoS_4$ precipitation mechanism predicts both the existence of asymptotes and their POC independence. Because asymptotes block quantitative Mo_{aq} precipitation, final $\delta^{98}Mo$ values in euxinic marine sediments are apt to be offset from those in seawater, but the difference is small in modern environments because $(Mo_{aq})_{asymptote} \ll (Mo_{aq})_{seawater}$. Asymptotes lie above the Mo_{aq} concentration believed to limit Mo nitrogenase biosynthesis, suggesting that without substantial acidification, global euxinia cannot deplete Mo_{aq} sufficiently to create marine nitrogen crises.

Existence and Characteristics of Asymptotes

In the oxic ocean, dissolved Mo (Mo_{aq}) is almost entirely MoO_4^{2-}. Particulate Mo (Mo_s) constitutes <0.001 % of ΣMo, except near terrigenous or hydrothermal particle sources (Ho et al., 2018). However, where H_2S or HS^- replaces dissolved O_2, MoO_4^{2-} becomes thiolated, and Mo_{aq} concentrations fall sharply toward asymptotes while Mo_s in contiguous sediments rises. The resulting elevated Mo_s is interpreted as signifying sulfide's presence during sedimentation.

A compilation in Table 1 shows that the span of Mo_{aq} asymptote concentrations in diverse sulfidic environments is remarkably narrow. Entries in Table 1 meet the criteria that (a) a water column or pore water becomes sulfidic at depth, (b) Mo_{aq} drops markedly (by >50 %) below where sulfide first appears, and (c) Mo_{aq} ultimately stabilises at asymptotes (designated $Mo_{aq,\infty}$) that are distinctly above analytical detection limits. The median asymptote value is 7.8 nM, and four fifths of the values fall in the range 2.5–13.3 nM. Asymptotes are prevalent in nature, but not universal; beneath some lakes and coastal embayments, pore water Mo_{aq} concentrations fall to minima before rising at greater depths (see Morford et al., 2009; Dahl et al., 2010; Havig et al., 2015; Sulu-Gambari et al., 2017). The reason for this atypical pattern is unclear; infiltration of groundwater from surrounding uplands or very slow reductive dissolution of Mo-rich detrital phases sourced from nearby land may be contributing factors.

Of particular importance in Table 1 is the million-fold range of particulate organic carbon (POC) concentrations (expressed per unit volume of solution). For instance, during diagenesis, solutes in Hingham Bay's sulfidic pore waters are in diffusive contact with ~1.5 moles POC/L (calculated for sediments with 3.2 % total organic carbon, porosity = 0.8, and 2.5 g/cm³ dry density; see Note II in the Supplementary Information). In contrast, measured POC concentrations in the Black Sea's sulfidic deep waters are 2.5–5.0 × 10⁻⁶ mol/L (Kaiser et al., 2017). Despite the 10⁶ difference, similar $Mo_{aq,\infty}$ asymptotes occur in both places. It could be argued that a mismatch in renewal rates of water and organic particles in the Black Sea makes this apparent POC disparity misleading. Below 1 km depth, the Black Sea's water is renewed every ~10³ yr whereas its POC is renewed every ~10¹ yr (estimated from the POC accumulation rate in underlying sediments; Arthur et al., 1994). Thus, deep water is *cumulatively* exposed to 10² times more POC than is present *instantaneously*. On this basis, the Black Sea's POC concentration is only 10⁴, rather than 10⁶, times smaller than Hingham Bay's, but the disparity is still huge.

Asymptotes are likewise insensitive to final S^{-II} concentrations (Table 1). For example, the maximum S^{-II} concentration in the Black Sea is 0.4 mM and that in Kyllaren Fjord is 5.0 mM, but both reach similar $Mo_{aq,\infty}$ asymptotes. The extreme $Mo_{aq,\infty}$ asymptotes in Table 1 (*i.e.* Walker Lake, 130 nM, and York River, 1.1 nM) mirror pH extremes, hinting that pH explains some of the asymptote variation, though the data are insufficient to establish this for certain. Any explanation for Mo_{aq} removal from sulfidic natural waters must account for why asymptotes are insensitive to ΣS^{-II} (= H_2S_{aq} + HS^-) and POC, but possibly sensitive to pH.

Departments of Geology and Chemistry, University of Maryland, College Park MD 20742, USA

*   Corresponding author (email: helz@umd.edu)

Table 1 Limits to the degree of dissolved Mo removal from sulfidic environments ($Mo_{aq,0}$ = dissolved Mo at onset of sulfidic conditions; $Mo_{aq,\infty}$ = dissolved Mo at asymptote; S^{-II} is total dissolved sulfide range over depths where $Mo_{aq,\infty} \approx$ constant). For sources of data, see Note I in the Supplementary Information.

Removal within:	pH	S^{-II} (mM)	Particulate POC* (mM)	$Mo_{aq,0}$ (nM)	$Mo_{aq,\infty}$ (nM)	$Mo_{aq,\infty}/Mo_{aq,0}$ (%)
Euxinic marine water columns						
Black Sea (1991)		0.30–0.41	0.0025	36	**2.6**	7
Black Sea (2011)	7.6	0.30–0.37		37	**7.8**	21
Black Sea (2017		0.35–0.42	0.0025–0.005	41	**5.9**	14
Black Sea (2019)	7.34	0.31–0.36		36	**6.9**	19
Framvaren Fjord	7.1	0.30–7.20	0.0027 ± 0.0006	50	**17.2**	34
Kyllaren Fjord		4.23–5.02	0.003–0.008	71	**7.5**	11
Rogoznica Lake (Sept.)	7.2	0.42–2.34	0.24 ± 0.10	97	**4.5**	5
Sulfidic pore waters						
Chesapeake Bay	7.2	1.15		55	**7.8**	14
Guaymas Basin (MUC9, >25 cm)		0.12–0.43	1580 ± 68	130	**12.3**	9
Hingham Bay (Oct. 2001, >7 cm)		0.49–1.01	1530 ± 79	112	**9.3**	8
Landsort Deep (LD 1)		1.73–2.09	2200 ± 900	26	**2.1**	8
Long Island Sound (FOAM, >20 cm)		2.5–3.3	680 ± 120	115	**13.3**	12
Storfjärden (Stn 3)		0.005–0.45	2100 ± 300	30	**8.**	27
Terrebonne Bay (9A)	7.0	0.09–1.61		33	**7.3**	22
Walker Lake (WL-2)	8.4	5.4–6.2	620–1100	5700	**134.**	2
York River groundwater	6.9	0.91–1.60		73	**1.1**	2
Euxinic lake water columns						
Fayetteville Green Lake	6.9	0.44–1.86	0.066	121	**13.2**	11
Lago Cadagno (Aug 2007)	7.1	0.10	0.0068	14	**2.5**	18
Lake Fryxell	7.5	0.30–1.20	0.062 ± 0.023	26	**3.5**	13
Mahoney Lake	7.4	35.0		230	**12.**	5
Median					**7.8**	12

*Particulate POC concentrations are expressed per litre of solution. Where more than three POC measurements are available, mean ± standard deviation is reported; otherwise, the range is given.

Organic Scavenging

The principal argument for organic scavenging rests on correlations commonly, but not universally, observed between Mo_s and organic matter in sedimentary rocks. As reviewed by Helz and Vorlicek (2019), no satisfactory molecular mechanism to explain Mo_{aq} scavenging by organic matter under natural conditions has yet been found, and evidence is also lacking for significant biological scavenging. If organic scavenging exists, it is likely to be an abiotic process that can be described by a Langmuir isotherm as:

$$\frac{Mo_s}{x_s POC} = \left[\frac{K_n' x_n}{1 + K_n' x_n Mo_{aq}}\right] Mo_{aq} \qquad \text{Eq. 1}$$

where Mo_s is non-lithogenic Mo adsorbed onto particulate organic carbon (mol Mo_s/L), x_s the mole fraction of a specific binding site (mol sites/mol C), POC the particulate organic carbon concentration (mol/L), K_n' the conditional binding constant (L/mol) for the nth $MoO_{4-n}S_n^{2-}$ ion, and x_n the mole fraction of the nth $MoO_{4-n}S_n^{2-}$ ion in Mo_{aq} (see Fig. 1).

For simplicity, Equation 1 assumes only one adsorbing $MoO_{4-n}S_n^{2-}$ species and only one binding site. Multiple species or sites could be included by adding more terms. At the pH and Mo_{aq} concentrations of most sulfidic natural waters, the second term in the denominator is negligible, making isotherms linear. In the linear case, Equation 1 is tantamount to the empirical

Mo_s/POC *vs.* Mo_{aq} relationship found for euxinic basin sediments by Algeo and Lyons (2006; see their Fig. 8a).

What does the linear form imply about aqueous asymptotes? Mass balance requires that:

$$Mo_{aq} = Mo_{aq,0} - Mo_s = Mo_{aq,0} - x_s POC[K_n' x_n]Mo_{aq} \qquad \text{Eq. 2}$$

where $Mo_{aq,0}$ is the initial total dissolved Mo and Mo_{aq} is the same during adsorption progress. Rearranging:

$$\frac{Mo_{aq}}{Mo_{aq,0}} = \frac{1}{1 + x_s POC[K_n' x_n]} \qquad \text{Eq. 3}$$

In diverse euxinic basins and sulfidic pore waters, asymptotes fix the ratio on the left hand side of this equation at a median value of 12 % (seventh column, Table 1). This requires that in nature the denominator's second term has a restricted range centred near 8. Given the 10^6 range of its POC factor, this requirement cannot possibly be met. Additionally, at any specific site, the ratio on the left is roughly constant through the asymptote zone, requiring that the second term in the denominator is also constant. However, H_2S_{aq} varies through asymptote zones (third column, Table 1), and x_n values strongly vary with H_2S_{aq} (Fig. 1). Only at high H_2S_{aq} concentrations, where x_4 becomes sulfide independent, can Equation 3 describe constant asymptotes at a constant POC concentration. (In this case, x_4 replaces x_n in Equation 3, implying that MoS_4^{2-} is the only adsorbed
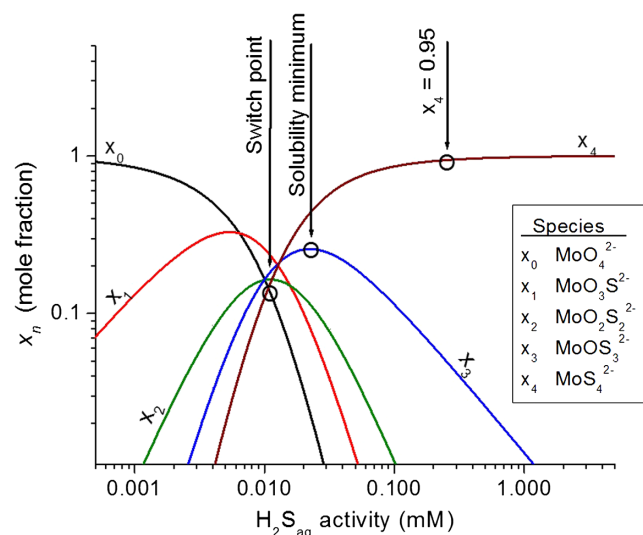
Figure 1 Mole fractions of aqueous $MoO_{4-n}S_n^{2-}$ species *versus* the activity of H_2S_{aq}, which is the non-ionised fraction of total dissolved sulfide. Circles mark three special points: where $MoO_4^{2-} = MoS_4^{2-}$ (switch point); where x_3 reaches its maximum (corresponding to the solubility minimum); and where $x_4 \geq 0.95$, signifying effective completion of Mo_{aq} thiolation.

Table 2 Concentrations of H_2S_{aq} (µM) at selected temperatures and degrees of MoO_4^{2-} thiolation (ionic strength = 0).

Temperature (°C)	Switch point ($MoO_4^{2-} = MoS_4^{2-}$)	Solubility minimum ($MoOS_3^{2-}$ peak)	$x_4 = 0.95$ (thiolation ≈ complete)
5	5	9	120
25	11	21	260
45	22	42	530
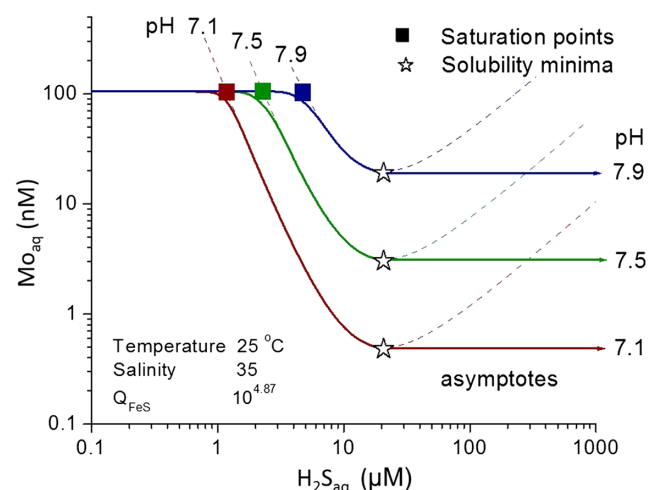
Figure 2 Effect of rising H_2S_{aq} on $FeMoS_4$ solubility (dashed curves) in seawater (initial $Mo_{aq} = 105$ nM) assuming saturation with FeS_{nano}, a material more soluble and reactive than mackinawite (Wolthers *et al.*, 2005; Matamoros-Veloza *et al.*, 2018). At $FeMoS_4$ saturation points (squares), the solubility drops below ambient $Mo_{aq,0}$ and precipitation begins. Eventually, solubility minima (stars) are reached. Actual Mo_{aq} follows the heavy curves because an irreversible redox transformation blocks redissolution of precipitated Mo. Based on Equation 2 in Helz and Vorlicek (2019).

species.) However, H_2S_{aq} concentrations high enough for x_4 to approach constancy exceed the concentrations at which Mo_{aq} asymptotes commence in nature. For example, the Mo_{aq} asymptote in the Black Sea commences at $H_2S_{aq} \approx 50$ µM (where $\Sigma S^{-II} \approx 300$ µM), whereas Figure 1 shows that H_2S_{aq} must be much higher, near 200 µM, for x_4 to come within 5 % of its ultimate limiting value. Equation 3, which describes organic scavenging, therefore cannot explain Mo_{aq} asymptotes.

FeMoS₄ Precipitation

Earlier workers rejected the possibility of Mo precipitation by sulfide. Emerson and Huested (1991) pointed out that, unlike sulfide-precipitated metals, Mo_{aq} fails to decline continuously with increasing ΣS^{-II}. In agreement, Algeo and Lyons (2006) noted that Cariaco Basin sediments accumulate higher Mo_s concentrations than Black Sea sediments, even though Cariaco waters contain less sulfide.

Nevertheless, Vorlicek *et al.* (2018) found a colloidal precipitate, $FeMoS_4$, with a solubility that could explain Mo_{aq} asymptotes in the Black Sea. At equilibrium with this precipitate (see derivation in Note III, Supplementary Information):

$$Mo_{aq} = \frac{10^{-19.83} 10^{2pH}}{Q_{FeS}(\gamma_{MoS_4})}(x_3)^{-1} \qquad \text{Eq. 4}$$

where γ_{MoS_4} is the activity coefficient of MoS_4^{2-} and $Q_{FeS} = \{Fe^{2+}\}\{H_2S_{aq}\}/\{H^+\}^2$. Except for the x_3 term, the factors on the righthand side of Equation 4 display limited variability in asymptote zones. Q_{FeS} values are usually constrained by saturation with iron monosulfide phases and pH is constrained mainly by strong $\Sigma CO_2/\Sigma ALK$ buffering. On the other hand, x_3 varies considerably, passing through a maximum with increasing H_2S_{aq} activity (Fig. 1). In Table 2, values of H_2S_{aq} at x_3 maxima have been estimated over a moderate temperature range by the isocoulombic extrapolation method (Gu *et al.*, 1994). Equation 4 requires that at x_3 maxima, Mo_{aq} solubility reaches minima; this is illustrated by dashed curves in Figure 2. However, aging transforms $FeMo^{VI}S_4$ to an inert Mo^{IV} phase, preventing Mo

redissolution when the solubility curves turn upward beyond the minima. As a result, the $FeMoS_4$ precipitation mechanism predicts that Mo_{aq} becomes fixed at asymptotes that are unresponsive to further H_2S_{aq} increases. The asymptotes are also independent of POC, despite the 10^6 range in nature, because organic matter has no role in the precipitation and aging reactions, except as fuel for biological sulfate reduction (Helz and Vorlicek, 2019). Thus $FeMoS_4$ precipitation meets the requirements listed above for a mechanism that can explain asymptotes.

Implications

Several implications of interest in the palaeoproxy field arise from this result.

Asymptotes block quantitative removal of Mo_{aq} from sulfidic waters, leaving dissolved residuals that ultimately escape the sulfidic environment. In the median case in Table 1, the residual ($Mo_{aq,\infty}/Mo_{aq,0}$) is only 12 % but can be much higher. This finding undermines the common assumption that marine euxinic basins preserve the $\delta^{98}Mo$ signatures of global seawater because of quantitative precipitation. Residuals will be greatest in waters of lower salinity, where $Mo_{aq,0}$ will be lower, and in

waters of higher pH, where $Mo_{aq,\infty}$ will be higher. Both situations generate higher $Mo_{aq,\infty}/Mo_{aq,0}$ ratios at asymptotes, permitting larger fractions of incoming Mo_{aq} to escape deposition.

The idea that Mo_s/POC ratios in sedimentary rocks can be used to estimate Mo_{aq} in ancient basins (Algeo and Lyons, 2006, and others) relies on the relationship in Equation 1, which is premised on the dominance of POC scavenging. Without scavenging, such Mo_{aq} estimates are ungrounded.

Table 1 shows that Mo_{aq} asymptotes in the pH range of modern environments all exceed 1 nM, the level thought to curb nitrogen fixation by Mo-nitrogenase (Glass *et al.,* 2010). Therefore, past global euxinia would not have shut down Mo-nitrogenase activity, creating marine nitrogen crises, unless accompanied by substantial acidification, which lowers $Mo_{aq,\infty}$ (Fig. 2).

Can $FeMoS_4$ precipitation explain why the Black Sea produces lower sedimentary Mo_s despite higher bottom water H_2S_{aq} concentrations compared to the Cariaco Basin? Consistent with the organic scavenging mechanism (Eq. 1), Algeo and Lyons (2006) regarded bottom water Mo_{aq} concentration, which is lower in the Black Sea, as the controlling variable. The Black Sea's lower bottom water Mo_{aq} concentration, and consequent lower sediment Mo_s concentration, were attributed to a Mo_{aq} supply restriction at the narrow Bosporus. This explanation is probably incorrect. The Bosporus distributes 4–5 times more Mo_{aq} into the Black Sea than its sediments accumulate (Piper and Calvert, 2009), and the excess returns through the Bosporus. On the other hand, the Bosporus restricts the Black Sea's river water throughput. Copious river inflow lowers surface salinity and intensifies density stratification, thus inhibiting introduction of oxidants into deep waters. Consequently, ΣS^{-II} accumulates sufficiently for the $FeMoS_4$ saturation point to ascend into the water column, causing Mo_{aq} drawdown there. Cariaco's better ventilation, attested by its shorter water residence time, suppresses ΣS^{-II} despite opposition from a greater POC rain rate. This confines Cariaco's saturation point to pore waters. Calculations based on ΣS^{-II} and pH data suggest that the Black Sea's saturation point is near 150 m depth in the water column, whereas Cariaco's is located a few mm below the sediment–water interface (Helz and Vorlicek, 2019). Therefore, Cariaco's bottom waters are pre-asymptote, whereas the Black Sea's are syn-asymptote. Cariaco's sediments accumulate more Mo_s by diffusion because of the very sharp, pre- to syn-asymptote Mo_{aq} gradient across the sediment–water interface.

To summarise, the narrow range of $Mo_{aq,\infty}$ values that form in sulfidic water columns and pore waters characterised by enormous differences in POC concentrations preclude adsorption to organic matter as an important Mo fixation process in nature. In contrast, $FeMoS_4$ precipitation, which depends on the thermodynamic activities of H^+, MoS_4^{2-}, and FeS rather than their concentrations, readily explains why Mo_{aq} asymptotes are independent of final sulfide and POC concentrations.

Editor: Liane G. Benning

Additional Information

Supplementary Information accompanies this letter at https://www.geochemicalperspectivesletters.org/article2129.

References

ALGEO, T.J., LYONS, T.W. (2006) Mo-total organic carbon covariation in modern marine environments: Implication for analysis of paleoredox and paleohydrographic conditions. *Paleooceanography and Paleoclimatology* 21, PA1016.

ARTHUR, M.A., DEAN, W.E., NEFF, E.D., HAY, B.J., KING, J., JONES, G. (1994) Varve calibrated records of carbonate and organic carbon accumulation over the last 2000 years in the Black Sea. *Global Biogeochemical Cycles* 8, 195–217.

DAHL, T.W., ANBAR, A.D., GORDON, G.W., ROSING, M.T., FREI, R., CANFIELD, D.E. (2010) The behavior of molybdenum and its isotopes across the chemocline and in the sediments of sulfidic Lake Cadagno, Switzerland. *Geochimica et Cosmochimica Acta* 74, 144–163.

EMERSON, S.R., HUESTED, S.S. (1991) Ocean anoxia and the concentrations of molybdenum and vanadium in seawater. *Marine Chemistry* 34, 177–196.

GLASS, J.B., WOLFE-SIMON, F., ELSER, J.J., ANBAR, A.D. (2010) Molybdenum-nitrogen co-limitation in freshwater and coastal heterocystous cyanobacteria. *Limnology and Oceanography* 55, 667–676.

GU, Y., GAMMONS, C.H., BLOOM, M.S. (1994) A one-term extrapolation method for estimating equilibrium constants of aqueous reactions at elevated temperatures. *Geochimica et Cosmochimica Acta* 58, 3545–3560.

HAVIG, J.R., MCCORMICK, M.L., HAMILTON, T.L., KUMP, L.R. (2015) The behavior of biologically important trace elements across the oxic/euxinic transition of meromictic Fayettville Green Lake, New York, USA. *Geochimica et Cosmochimica Acta* 165, 389–406.

HELZ, G.R., VORLICEK, T.P. (2019) Precipitation of molybdenum from euxinic waters and the role of organic matter. *Chemical Geology* 509, 178–193.

HO, P., LEE, J.-M., HELLER, M.I., LAM, P.J., SHILLER, A.M. (2018) The distributions of dissolved and particulate Mo and V along the U.S. GEOTRACES East Pacific zonal transect (GP16): The roles of oxides and biogenic particles in their distribution in the oxygen deficient zone and the hydrothermal plume. *Marine Chemistry* 201, 242–255.

KAISER, D., KONOVALOV, S., SCHULZ-BULL, D.E., WANIEK, J.J. (2017) Organic matter along longitudinal and vertical gradients in the Black Sea. *Deep Sea Research Part I* 129, 22–31.

MATAMOROS-VELOZA, A., CESPEDES, O., JOHNSON, B.R.G., STAWSKI, T.M., TERRANOVA, U., DE LEEUW, N.H., BENNING, L.G. (2018) A highly reactive precursor in the iron sulfide system. *Nature Communications* 9, 3125.

MORFORD, J.L., MARTIN, W.R., KALNEJAIS, L.H., FRANÇOIS, R., BOPTHNER, M., KARLE, I.-M. (2007) Insights on geochemical cycling of U, Re and Mo from seasonal sampling in Boston Harbor, Massachusetts, USA. *Geochimica et Cosmochimica Acta* 71, 895–915.

MORFORD, J.L., MARTIN, W.R., FRANÇOIS, R., CARNEY, C.M. (2009) A model for uranium, rhenium and molybdenum diagenesis in marine sediments based on results from coastal locations. *Geochimica et Cosmochimica Acta* 73, 2938–2960.

PIPER, D.Z., CALVERT, S.E. (2009 A marine biogeochemical perspective on black shale deposition. *Earth-Science Reviews* 95, 63–96.

ROLISON, J.M., STIRLING, C.H., MIDDAG, R., RIJKENBERG, M.J.A. (2017) Uranium stable isotope fractionation in the Black Sea: Modern calibration of the $^{238}U/^{235}U$ paleo-redox proxy. *Geochimica et Cosmochimica Acta* 203, 69–88.

SULU-GAMBARI, R., ROEPERT, A., JILBERT, T., HAGENS, M., MEYSMAN, F.J.R., SLOMP, C.P. (2017) Molybdenum dynamics in sediments of a seasonally-hypoxic coastal marine basin. *Chemical Geology* 466, 627–640.

VORLICEK, T.P., HELZ, G.R., CHAPPAZ, A., VUE, P., VEZINA, A., HUNTER, W. (2018) Molybdenum burial mechanism in sulfidic sediments: iron-sulfide pathway. *ACS Earth and Space Chemistry* 2, 565–576.

WOLTHERS, M., CHARLET, L., VAN DER LINDE, P.R., RICKARD, D., VAN DER WEIJDEN, C.H. (2005) Surface chemistry of disordered mackinawite (FeS). *Geochimica et Cosmochimica Acta* 69, 3469–3481.